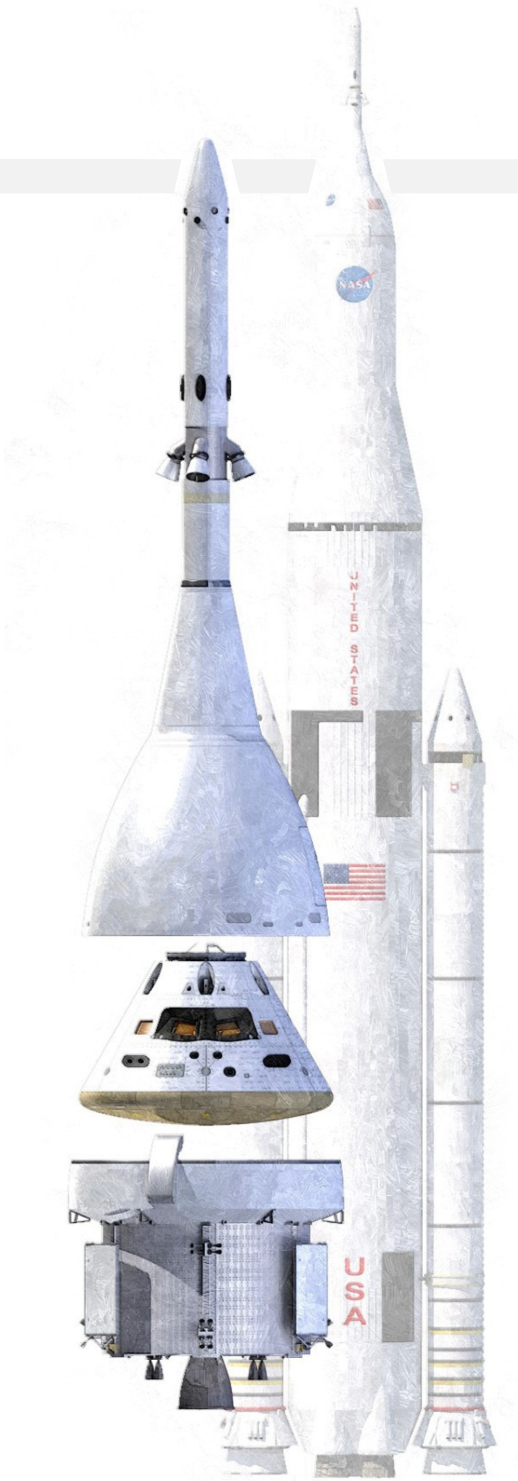

3D Material Response Analysis of PICA Pyrolysis Experiments

9th Ablation Workshop
August, 2017

A. Brandon Oliver
brandon.oliver-1@nasa.gov

Introduction

- Primarily interested in improving ablation modeling for use in inverse reconstruction of flight environments on ablative heatshields
  - Ablation model is essentially a component of the heat flux sensor, so model uncertainties lead to measurement uncertainties
  - Non-equilibrium processes have been known to be significant in low density ablators for a long time, but increased accuracy requirements of the reconstruction process necessitates incorporating this physical effect

- Attempting to develop a pyrolysis model for implementation in material response based on the PICA data produced by Bessire and Minton
  - Pyrolysis gas species molar yields as a function of temperature and heating rate

- Several problems encountered while trying to fit Arrhenius models to the data led to further investigation of the experimental setup

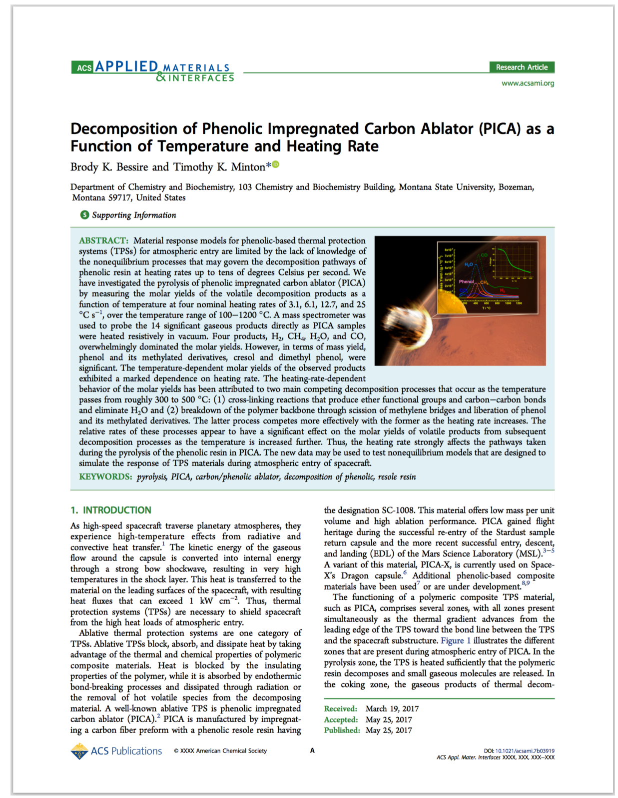

ACS APPLIED MATERIALS & INTERFACES

Research Article

www.acsami.org

Decomposition of Phenolic Impregnated Carbon Ablator (PICA) as a Function of Temperature and Heating Rate

Brody K. Bessire and Timothy K. Minton*

Department of Chemistry and Biochemistry, 103 Chemistry and Biochemistry Building, Montana State University, Bozeman, Montana 59717, United States

Supporting Information

ABSTRACT: Material response models for phenolic-based thermal protection systems (TPSs) for atmospheric entry are limited by the lack of knowledge of the nonequilibrium processes that may govern the decomposition pathways of phenolic resin at heating rates up to tens of degrees Celsius per second. We have investigated the pyrolysis of phenolic impregnated carbon ablator (PICA) by measuring the molar yields of the volatile decomposition products as a function of temperature at four nominal heating rates of 3.1, 6.1, 12.7, and 25 °C s^{-1}, over the temperature range of 100−1200 °C. A mass spectrometer was used to probe the 14 significant gaseous products directly as PICA samples were heated resistively in vacuum. Four products, H_2, CH_4, H_2O, and CO, overwhelmingly dominated the molar yields. However, in terms of mass yield, phenol and its methylated derivatives, cresol and dimethyl phenol, were significant. The temperature-dependent molar yields of the observed products exhibited a marked dependence on heating rate. The heating-rate-dependent behavior of the molar yields has been attributed to two main competing decomposition processes that occur as the temperature passes from roughly 300 to 500 °C: (1) cross-linking reactions that produce ether functional groups and carbon−carbon bonds and eliminate H_2O and (2) breakdown of the polymer backbone through scission of methylene bridges and liberation of phenol and its methylated derivatives. The latter process competes more effectively with the former as the heating rate increases. The relative rates of these processes appear to have a significant effect on the molar yields of volatile products from subsequent decomposition processes as the temperature is increased further. Thus, the heating rate strongly affects the pathways taken during the pyrolysis of the phenolic resin in PICA. The new data may be used to test nonequilibrium models that are designed to simulate the response of TPS materials during atmospheric entry of spacecraft.

KEYWORDS: *pyrolysis, PICA, carbon/phenolic ablator, decomposition of phenolic, resole resin*

1. INTRODUCTION

As high-speed spacecraft traverse planetary atmospheres, they experience high-temperature effects from radiative and convective heat transfer.[1] The kinetic energy of the gaseous flow around the capsule is converted into internal energy through a strong bow shockwave, resulting in very high temperatures in the shock layer. This heat is transferred to the material on the leading surfaces of the spacecraft, with resulting heat fluxes that can exceed 1 kW cm^{-2}. Thus, thermal protection systems (TPSs) are necessary to shield spacecraft from the high heat loads of atmospheric entry.

Ablative thermal protection systems are one category of TPSs. Ablative TPSs block, absorb, and dissipate heat by taking advantage of the thermal and chemical properties of polymeric composite materials. Heat is blocked by the insulating properties of the polymer, while it is absorbed by endothermic bond-breaking processes and dissipated through radiation or the removal of hot volatile species from the decomposing material. A well-known ablative TPS is phenolic impregnated carbon ablator (PICA).[2] PICA is manufactured by impregnating a carbon fiber preform with a phenolic resole resin having the designation SC-1008. This material offers low mass per unit volume and high ablation performance. PICA gained flight heritage during the successful re-entry of the Stardust sample return capsule and the more recent successful entry, descent, and landing (EDL) of the Mars Science Laboratory (MSL).[3−5] A variant of this material, PICA-X, is currently used on Space-X's Dragon capsule.[6] Additional phenolic-based composite materials have been used[7] or are under development.[8,9]

The functioning of a polymeric composite TPS material, such as PICA, comprises several zones, with all zones present simultaneously as the thermal gradient advances from the leading edge of the TPS toward the bond line between the TPS and the spacecraft substructure. Figure 1 illustrates the different zones that are present during atmospheric entry of PICA. In the pyrolysis zone, the TPS is heated sufficiently that the polymeric resin decomposes and small gaseous molecules are released. In the coking zone, the gaseous products of thermal decom-

Received: March 19, 2017
Accepted: May 25, 2017
Published: May 25, 2017

DOI: 10.1021/acsami.7b03919
ACS Appl. Mater. Interfaces XXXX, XXX, XXX−XXX

B. K. Bessire, T. K. Minton, "Decomposition of Phenolic Impregnated Carbon Ablator (PICA) as a Function of Temperature and Heating Rate", ACS Applied Materials & Interfaces 9 (25) (2017)

Data Overview

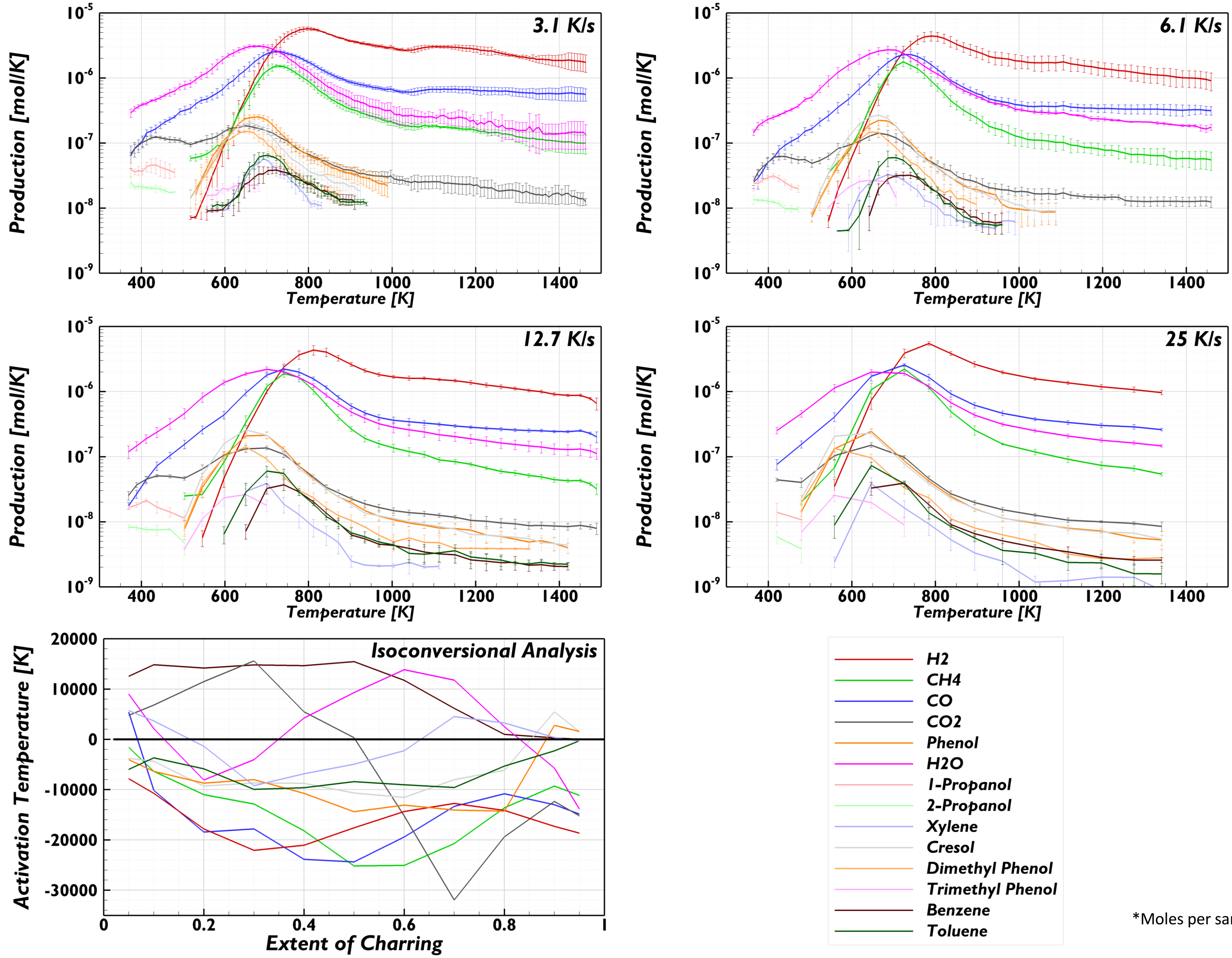

*Moles per sample volume

Difference in General "Shape" of Data

- Data for most species shows a tendency to rise at different temperatures and peak at similar temperature
- Model predictions generally rise together and peak at different times

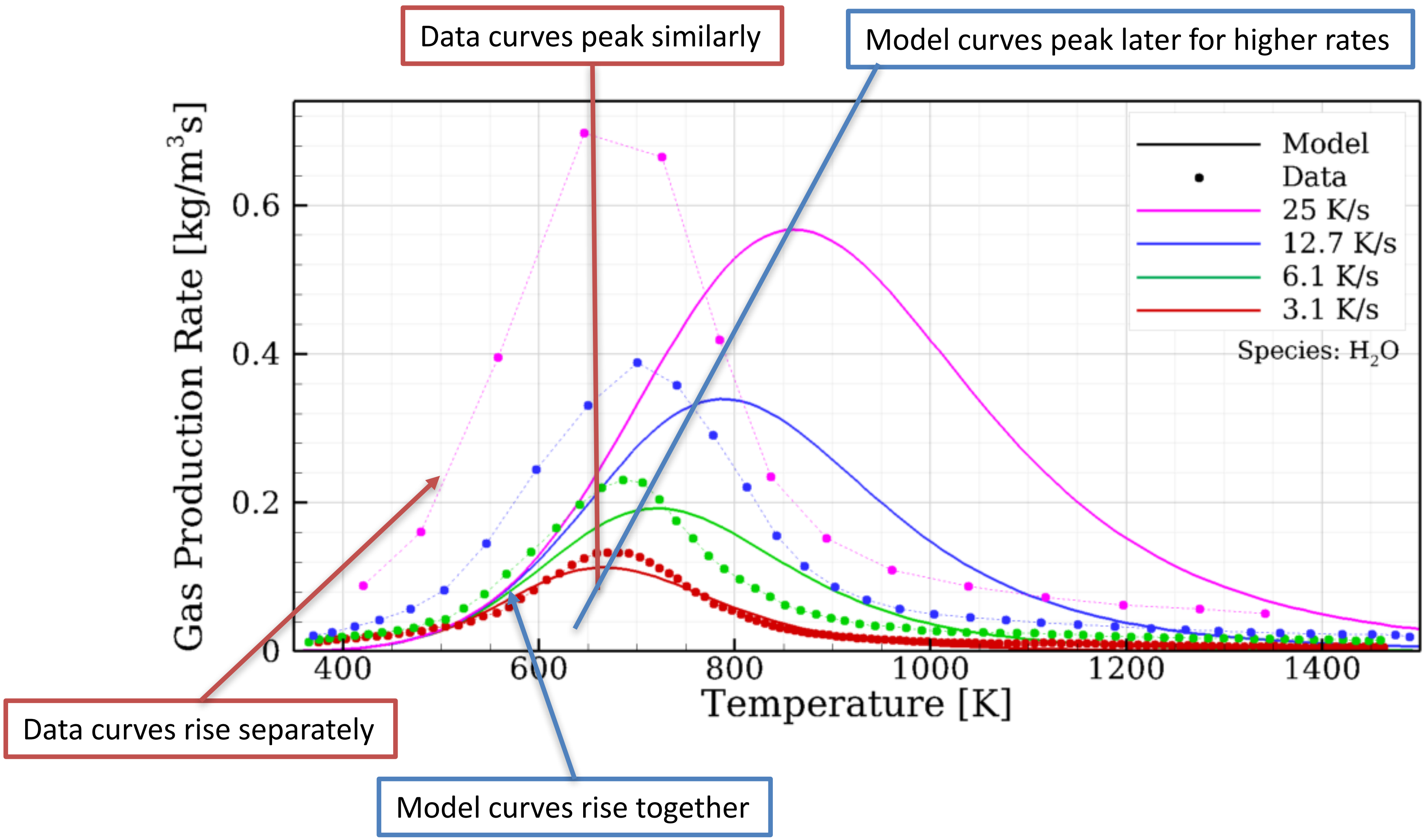

Difference in General "Shape" of Data

Have been unable to find model parameters that match the general shape of the data

$$\frac{\partial \rho_k}{\partial t} = \frac{M_k}{1000}\left(AT^{\psi}e^{-Ea/T}\right)\tilde{\rho}_k^{\theta'}$$

$\tilde{\rho}_k$: Molar Density

A : Rate constant

ψ : Temperature order

Ea : Activation Temperature

θ' : Reaction order

M_k : Molecular weight

$\frac{\partial \rho_k}{\partial t}$: Gas production rate

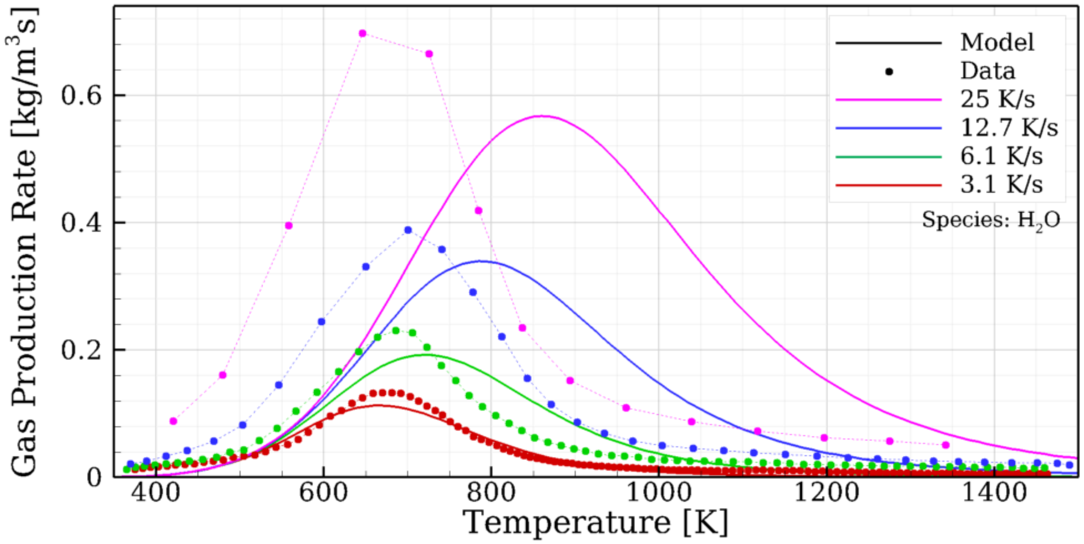

$\bar{\rho}_0 = 10.529\ \mathrm{kg/m^3}$

$A = 0.322$

$\psi = 0$

$Ea = 4600$

$\theta' = 1.7$

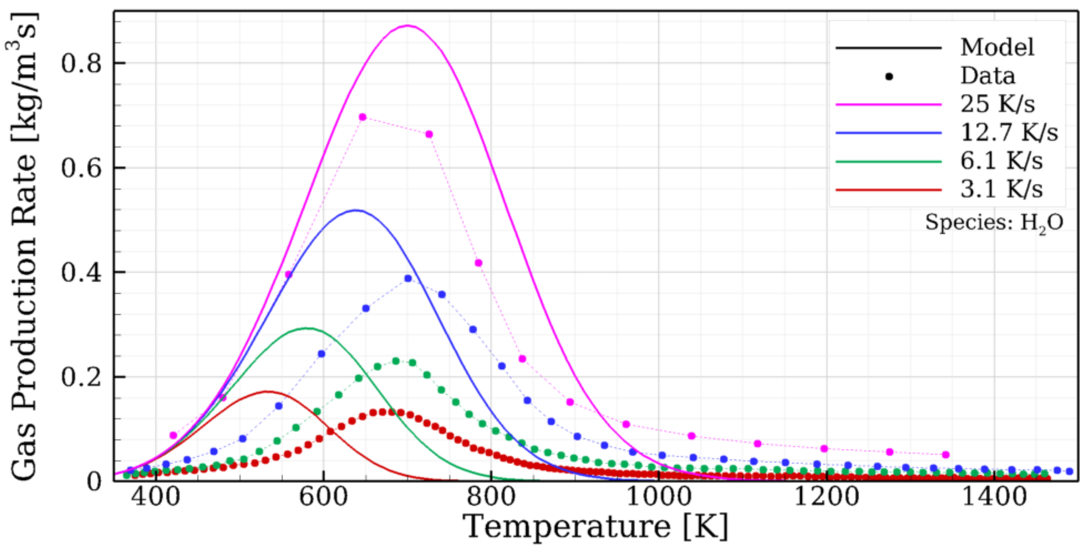

$\bar{\rho}_0 = 10.529\ \mathrm{kg/m^3}$

$A = 0.00933$

$\psi = 1.0$

$Ea = 2950$

$\theta' = 1.1$

General "Shape" of Data

Two identified possibilities:

- Model form is incorrect
  - Arrhenius models may not apply for long polymer chains with limited mobility and react with themselves?
  - Competitive reaction mechanism
- Data is being misinterpreted
  - Possible non-uniformities leading to more complicated behavior

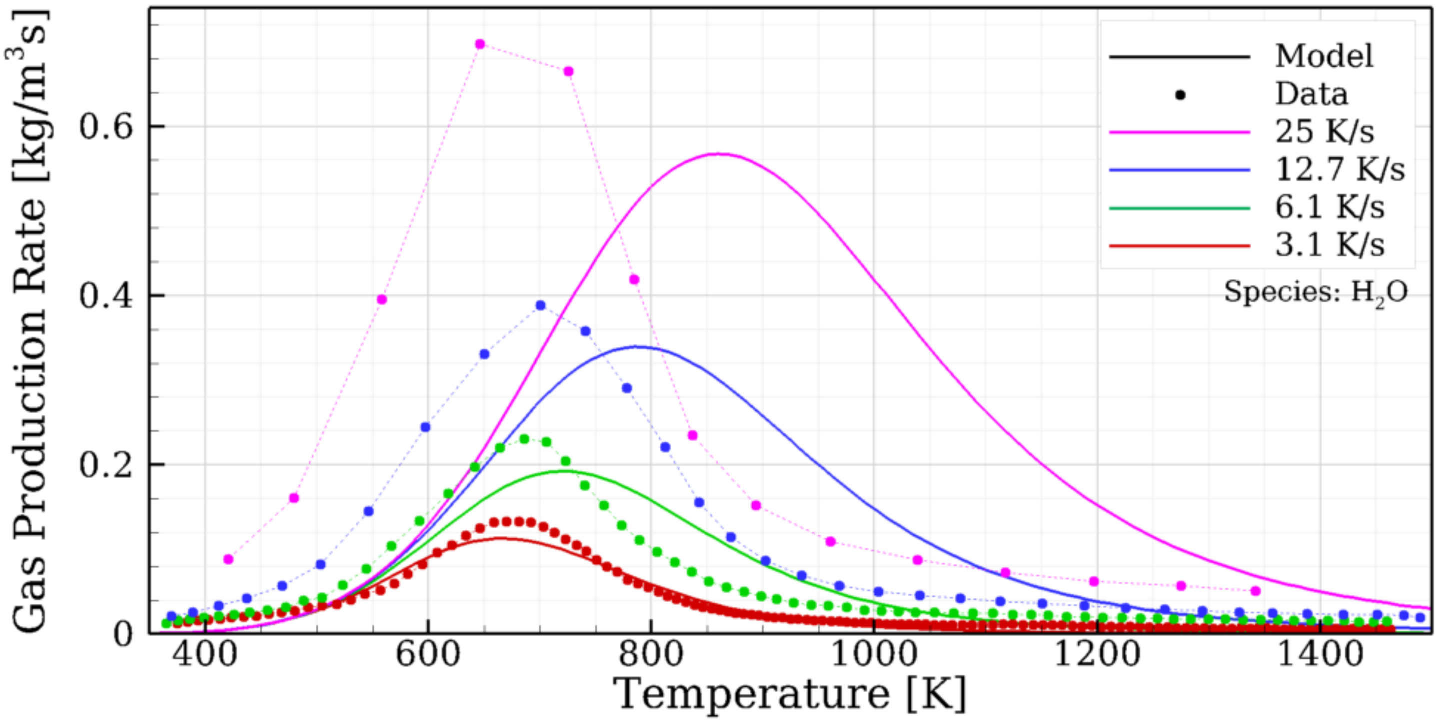

Sensitivity to Heating Rate Non-Uniformity

- Small non-uniformities in heating rate are present

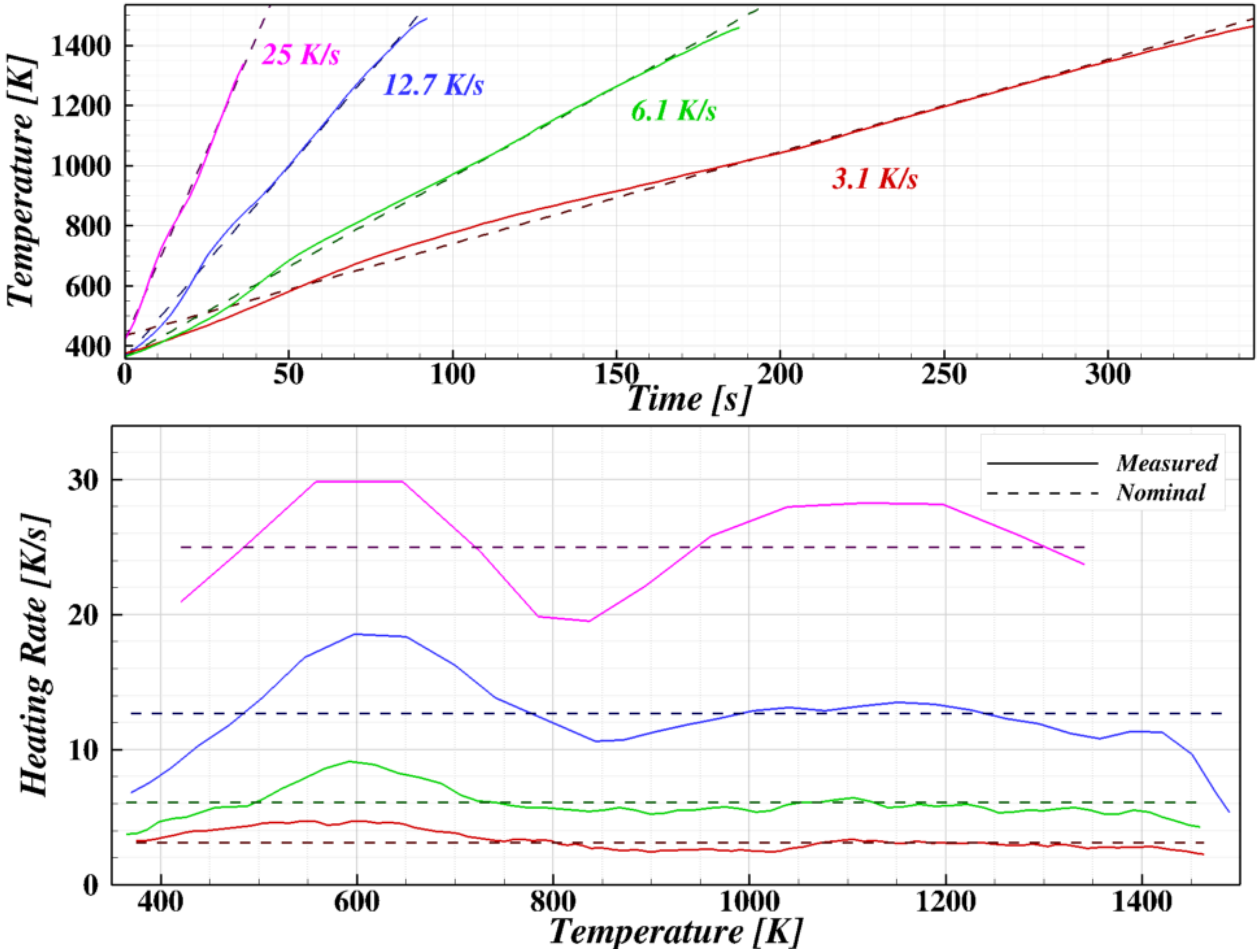

Sensitivity to Heating Rate Non-Uniformity

- Decomposition model is somewhat sensitive to non-uniformities in heating rate
  - Effect brings peaks closer into line, but it does not separate the curves in the rise to the peak
  - Integrating each individual temperature profile and averaging the result does not significantly change the result.

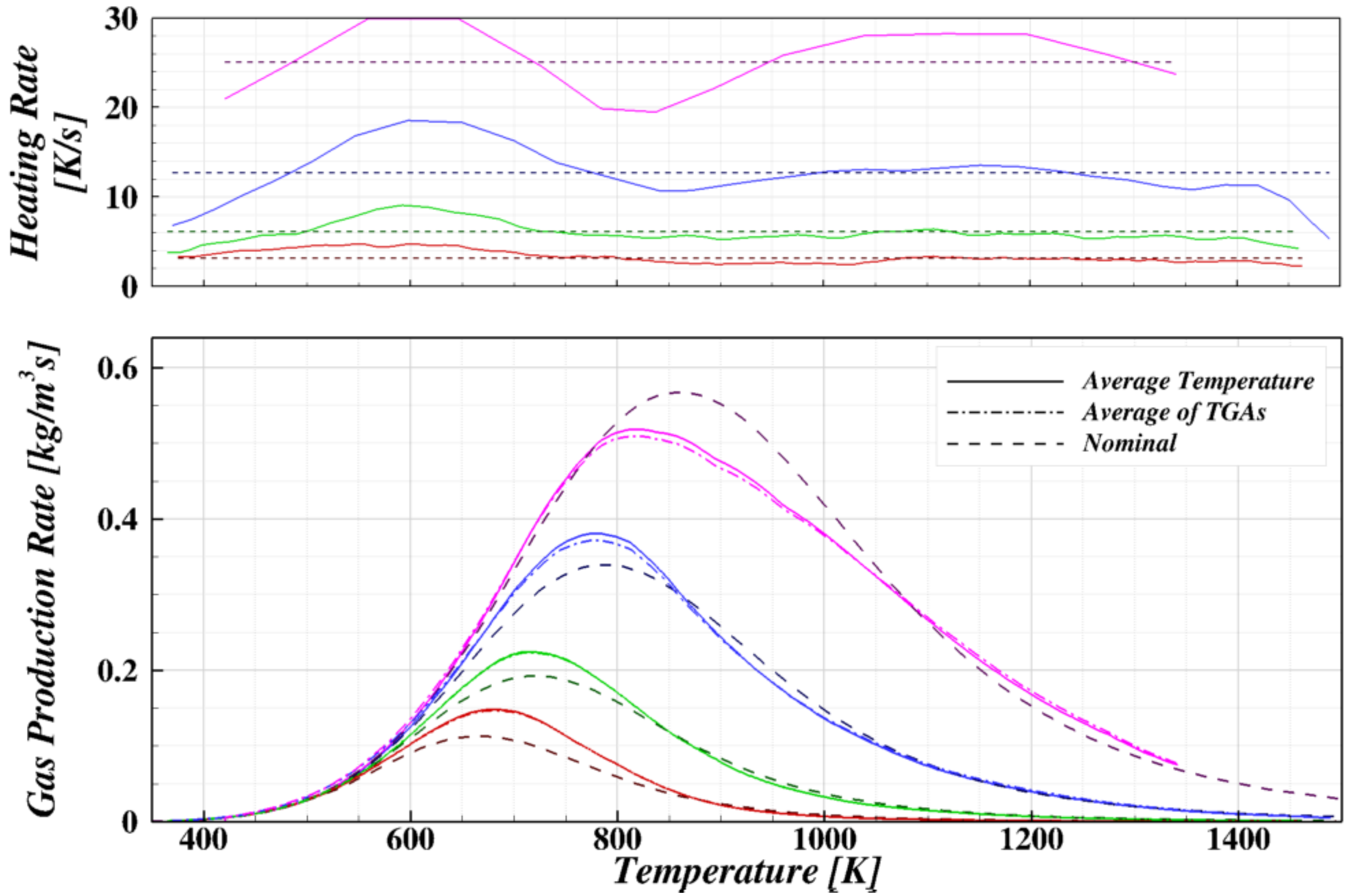

Spatial Non-Uniformity in Specimen

- 3 possible sources for spatial non-uniformity:
  1. Cooled clamps lead to parabolic profile along sample long-axis (noted in paper)
  2. Thermal radiation from all exposed surfaces leads to cooler temperature at surface than at center of sample
  3. Thermocouple measuring sample temperature locally cools sample by conducting heat down TC wires
     - Twisted-wire junction introduces uncertainty as to where the 'effective' junction is located
     - Contact resistance between wire and PICA
- Assess the potential impact of these effects with a 3D thermal analysis
  - Thermoelectric equations added to the CHAR code for this analysis
    - Joule heating of sample
    - Seebeck term for thermocouple modeling

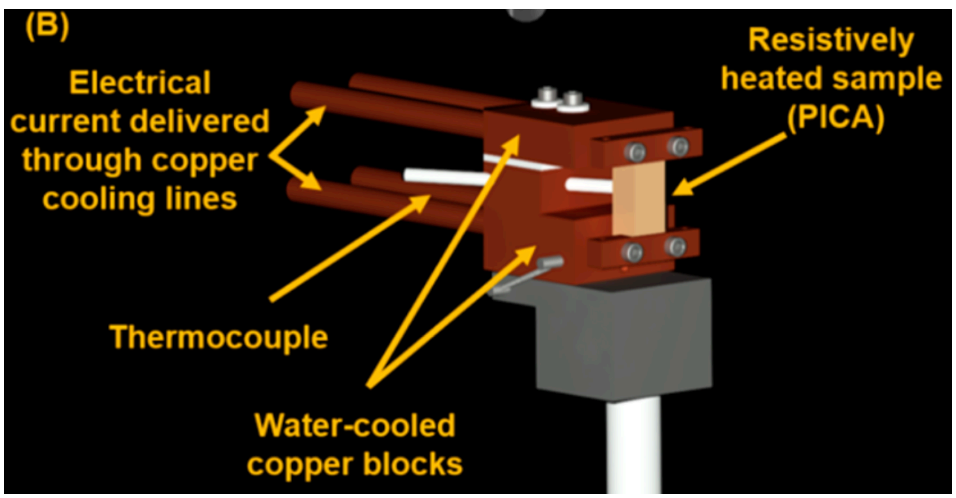

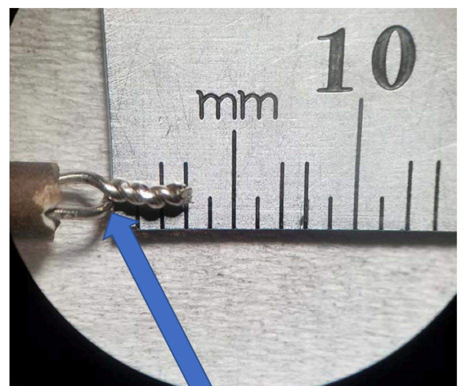

Thermocouple is inserted until last twist is just below the surface of the sample.

Depth of thermocouple in the sample is 3 mm.

Images courtesy of Tim Minton and Brody Bessire

Twisted TC Analysis

- Positive and negative leads of the type-K thermocouple span the space from the surface to the center of the specimen
  - Modeled TC wires with round (touching at one point) or square (touching for whole side) cross-sections to bound range of actual configuration
- Effective junction appears to be very close to the exposed surface of the sample
  - “TC Reading” indicates temperature inferred from voltage at end TC lead wires
  - Very little difference between square and round cross-section

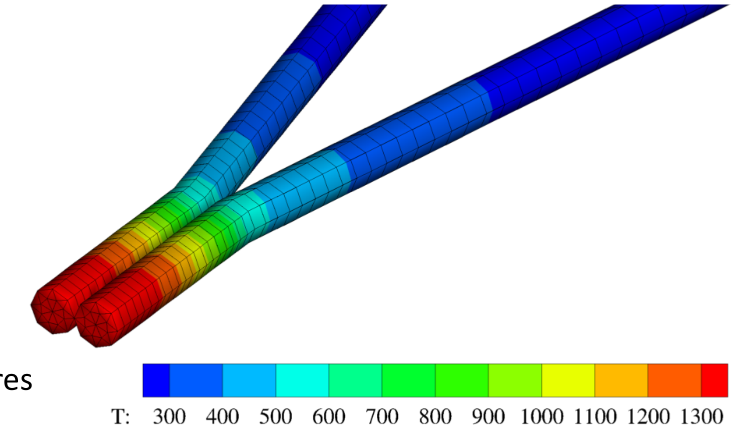

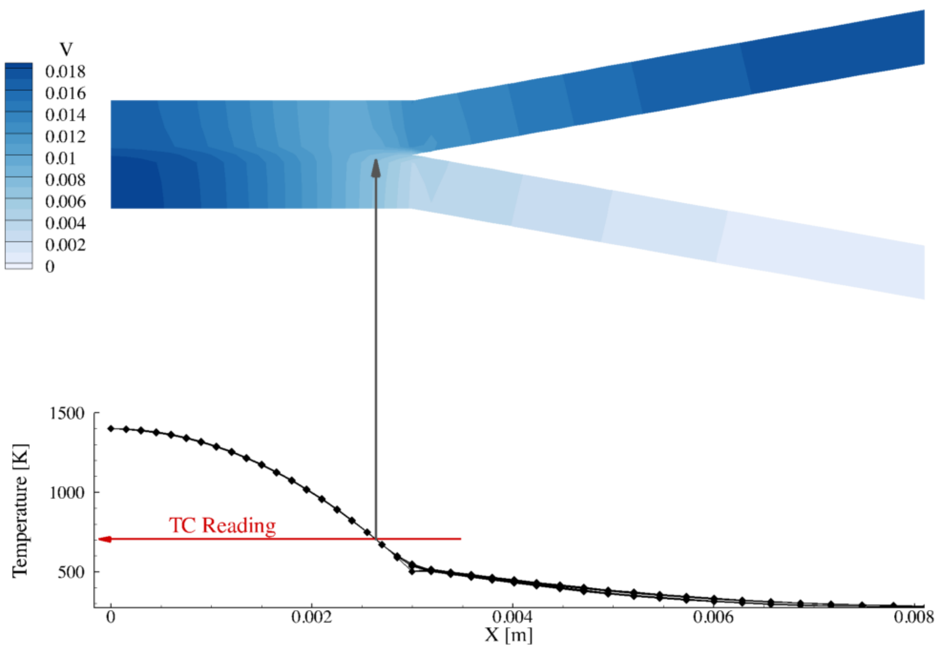

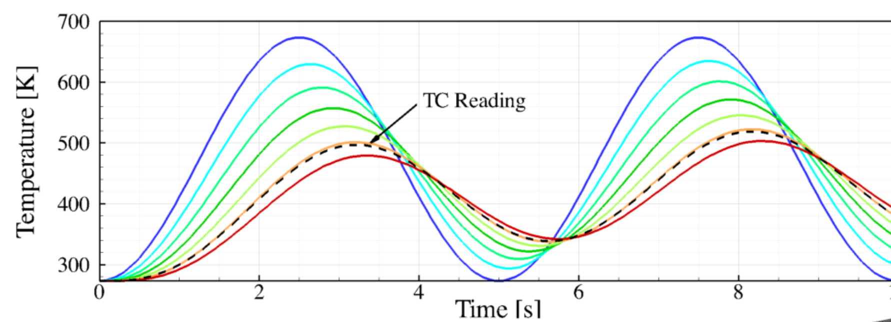

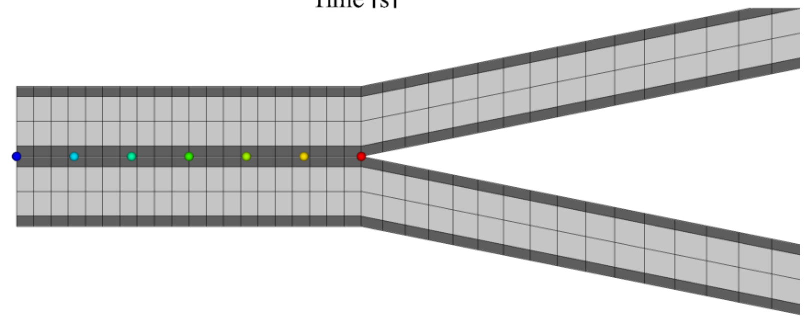

3D CHAR Model of Specimen

- ¼ Symmetry 3D model built of test specimen
  - TC wire assumed un-twisted, with square cross-section with same area as round wire
  - Wire assumed in perfect contact with PICA, adiabatic on all external boundaries
  - PICA exposed faces reradiate to 300K sink with view factor of 0.92 (account for some reflection back from copper fixture)
  - Temperature (300K) and voltage specified where copper electrodes contact specimen
    - Voltage boundary condition determined via DAKOTA parameter estimation to yield reported temperature at "Control TC" location
  - Temperatures at an array of points extracted and used to evaluate average gas production throughout sample

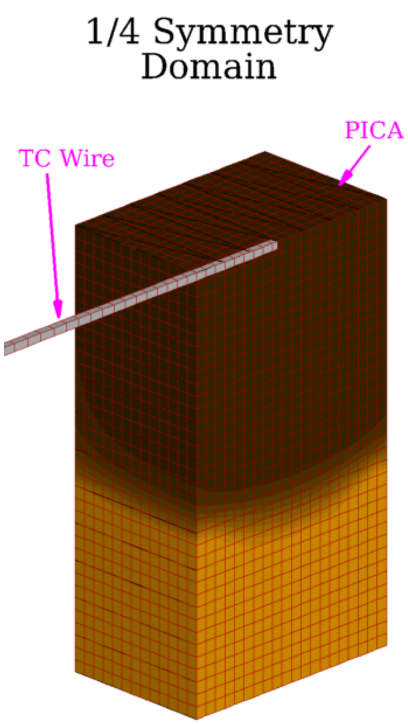

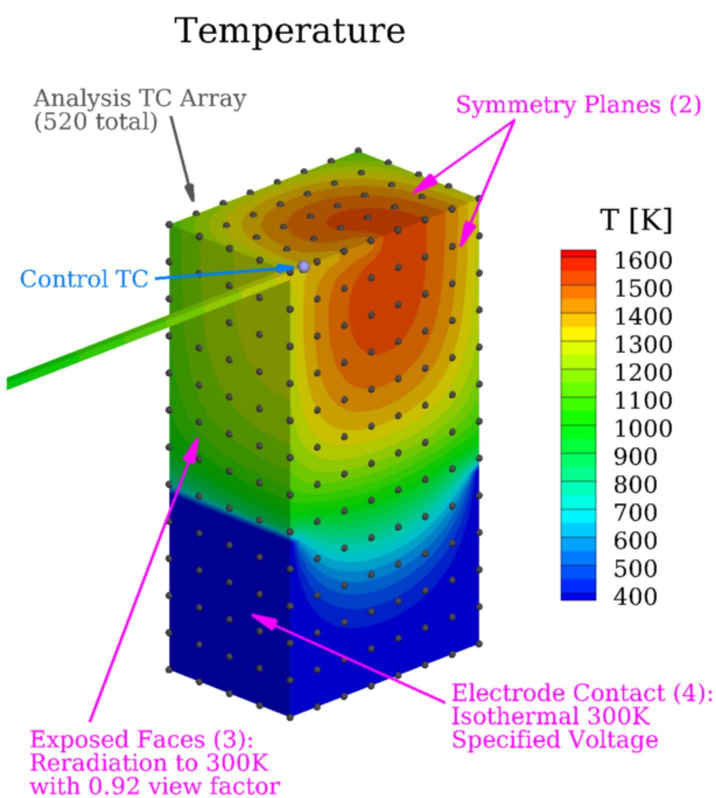

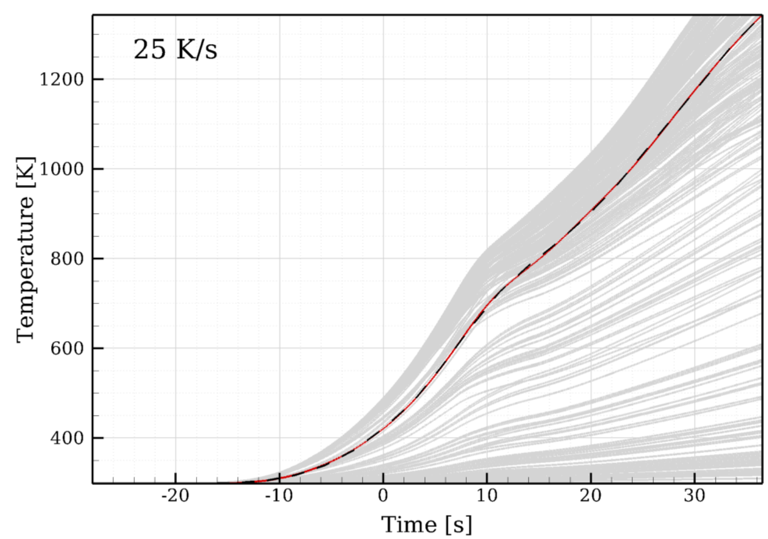

3D CHAR Simulation Caveats

Key limitations:

- PICA electrical resistivity assumed to follow graphite numbers obtained online (no difference between virgin and char)
  - Conductivity of graphite considered because believe trend will reduce non-uniformity
    - Heating proportional to resistivity, so heating will be somewhat reduced at elevated temperatures

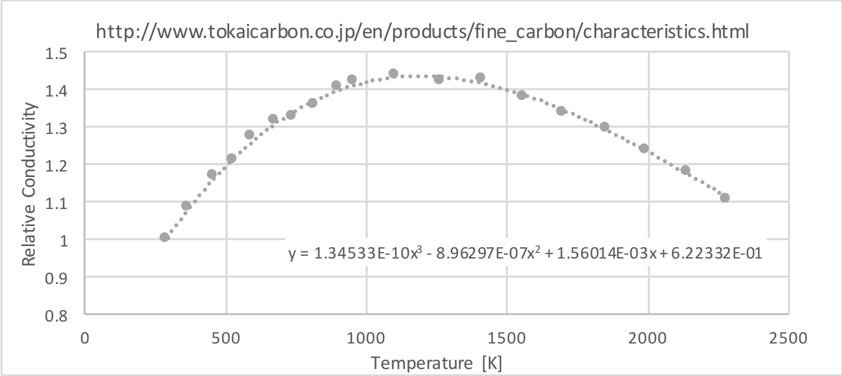

- PICA decomposition model heat of pyrolysis
  - Based on MSL flight data driver-TC analysis, the model is reasonably accurate; however I did not test sensitivity to this

- Thermal radiation reflectance from chamber modeled by 0.92 view factor
  - Rough calculation of net absorbance considering reflections from copper fixture

- Not considering likely contact resistance between TC and PICA
  - Sensitivity analysis shows that contact resistance significantly affects the results

Spatial Non-Uniformity in Specimen

- Average TGA response over the entire specimen volume calculated from CHAR TC array results
    1. Average temperatures in each “cell” of the TC matrix (336 total)
    2. Compute species production rate (given a model) for each cell
    3. Average the species production rates over all cells
    4. Plot average production rate vs control TC temperature

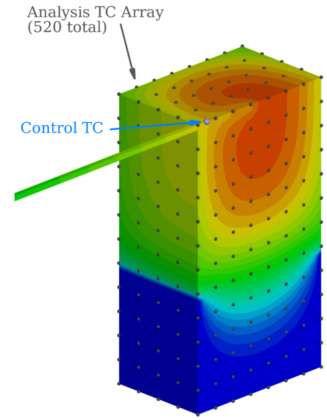

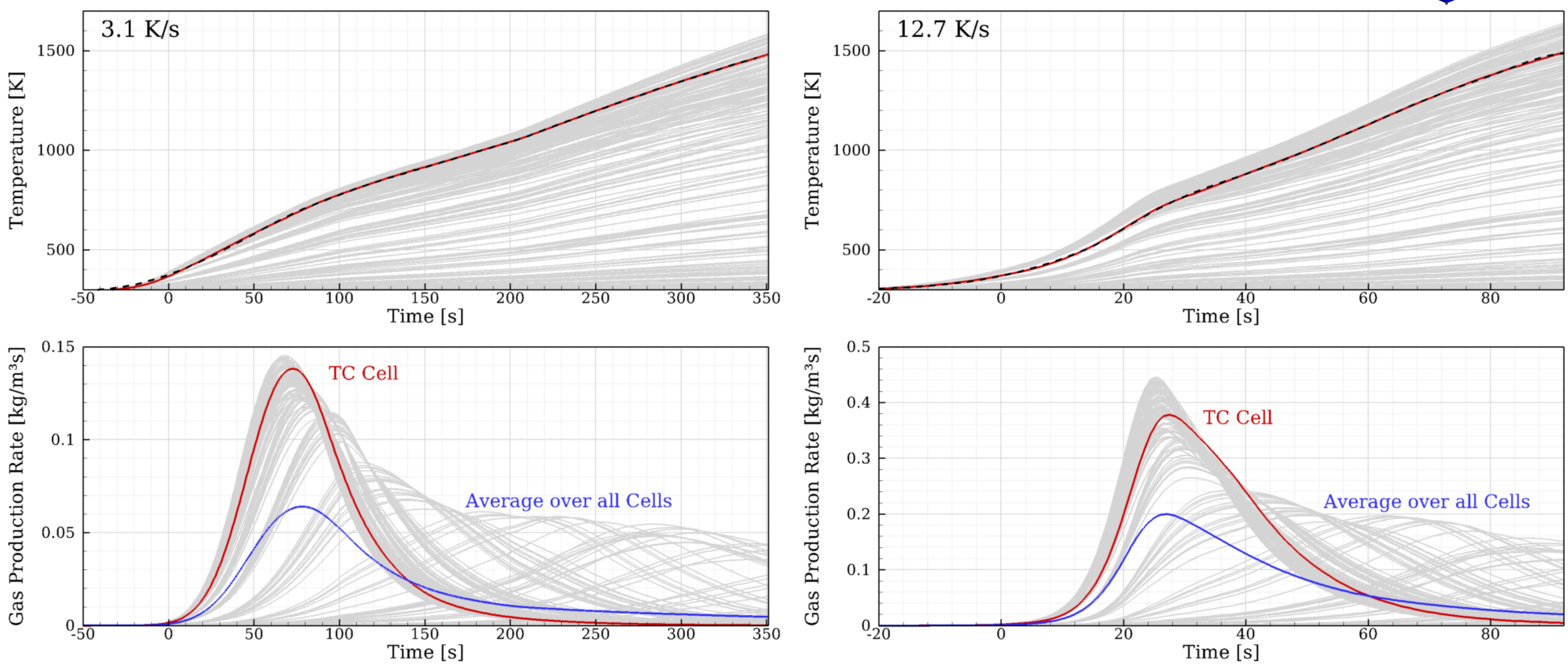

Spatial Non-Uniformity in Specimen

- Averaging the TGA response over the entire sample volume yields desired shift in gas production rate
- Shift amount is likely dependent on modeling assumptions
  - Expect that more accurate electrical conductivity model for PICA would change results
  - TC contact resistance does change results
- Different reaction model is required to get volume averaged production rate to match data

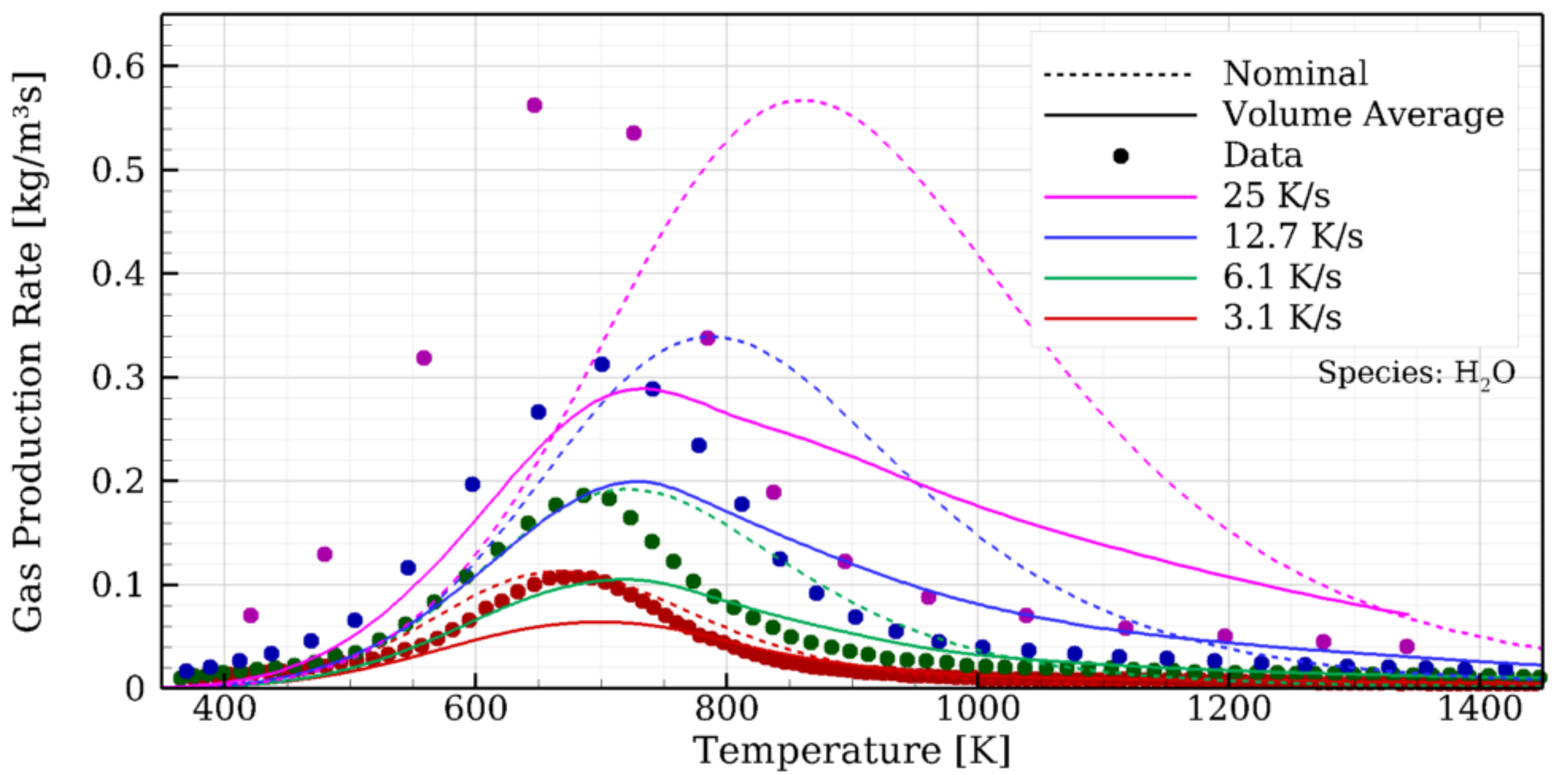

Spatial Non-Uniformity in Specimen

- Particle-swarm optimization used to determine reaction model to better fit data with volume averaged TGA
- Still not quite capturing everything, and some other species are horribly mis-predicted. Possible causes:
  - Incorrect temperature distribution throughout sample
  - Non-competitive reaction mechanism used here (Bessire & Minton suggest that mechanism should be competitive)

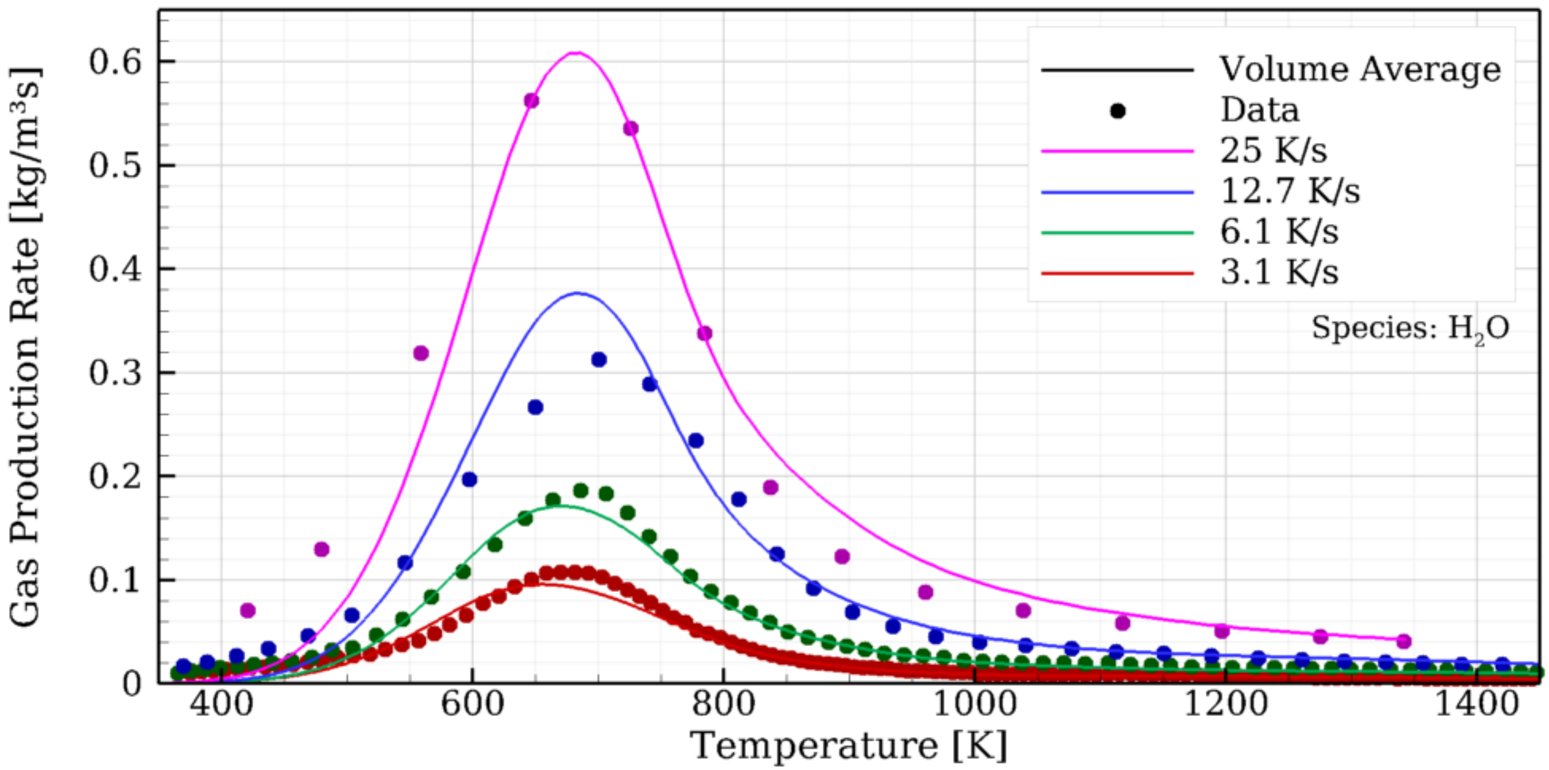

Non-Competitive Mechanism Results

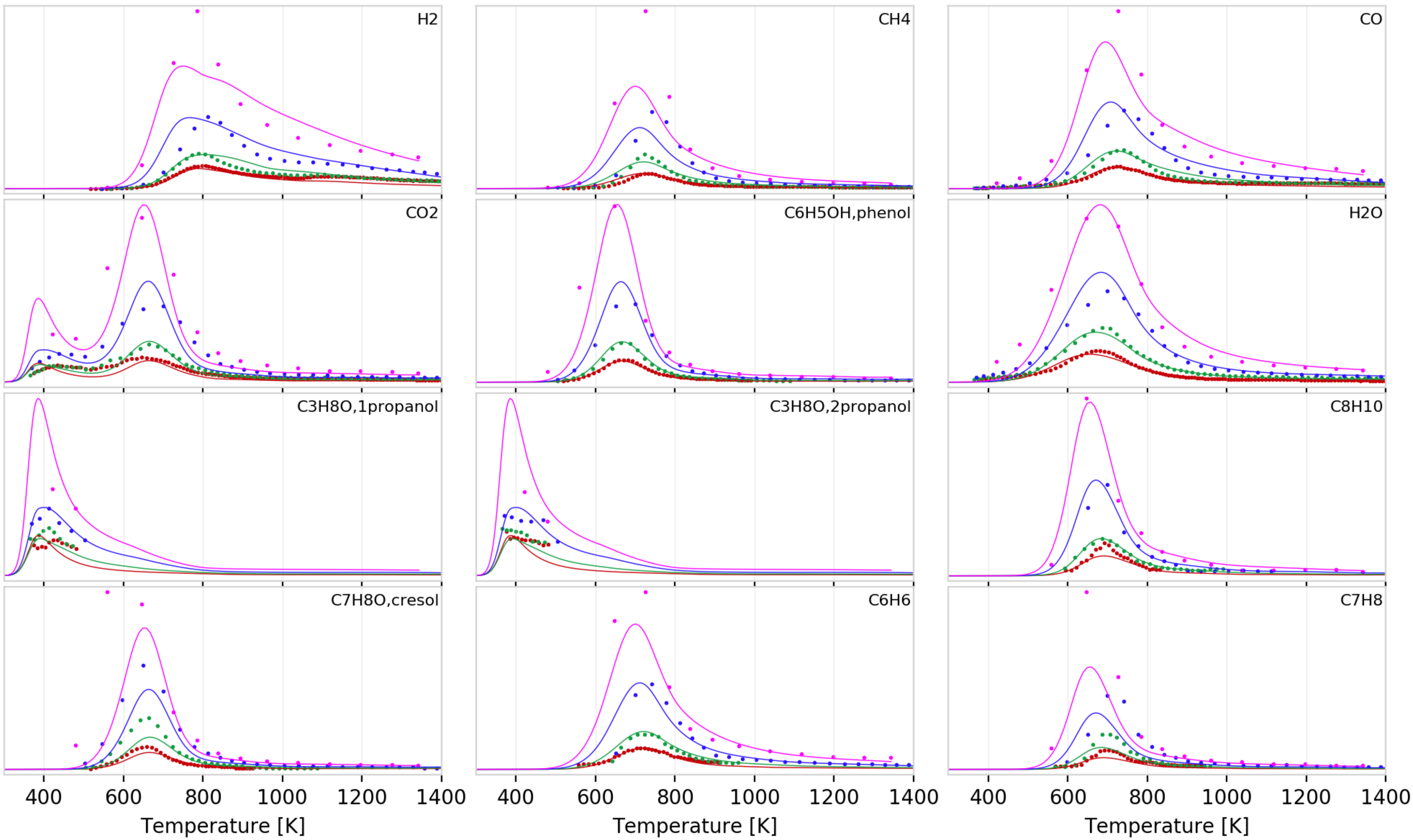

TC Contact Conductance

- Including contact conductance enhances movement of gas production peaks
- Assumed value appears to be too large (or the assumption of non-competitive reactions is very poor)
  - Other species perform very poorly

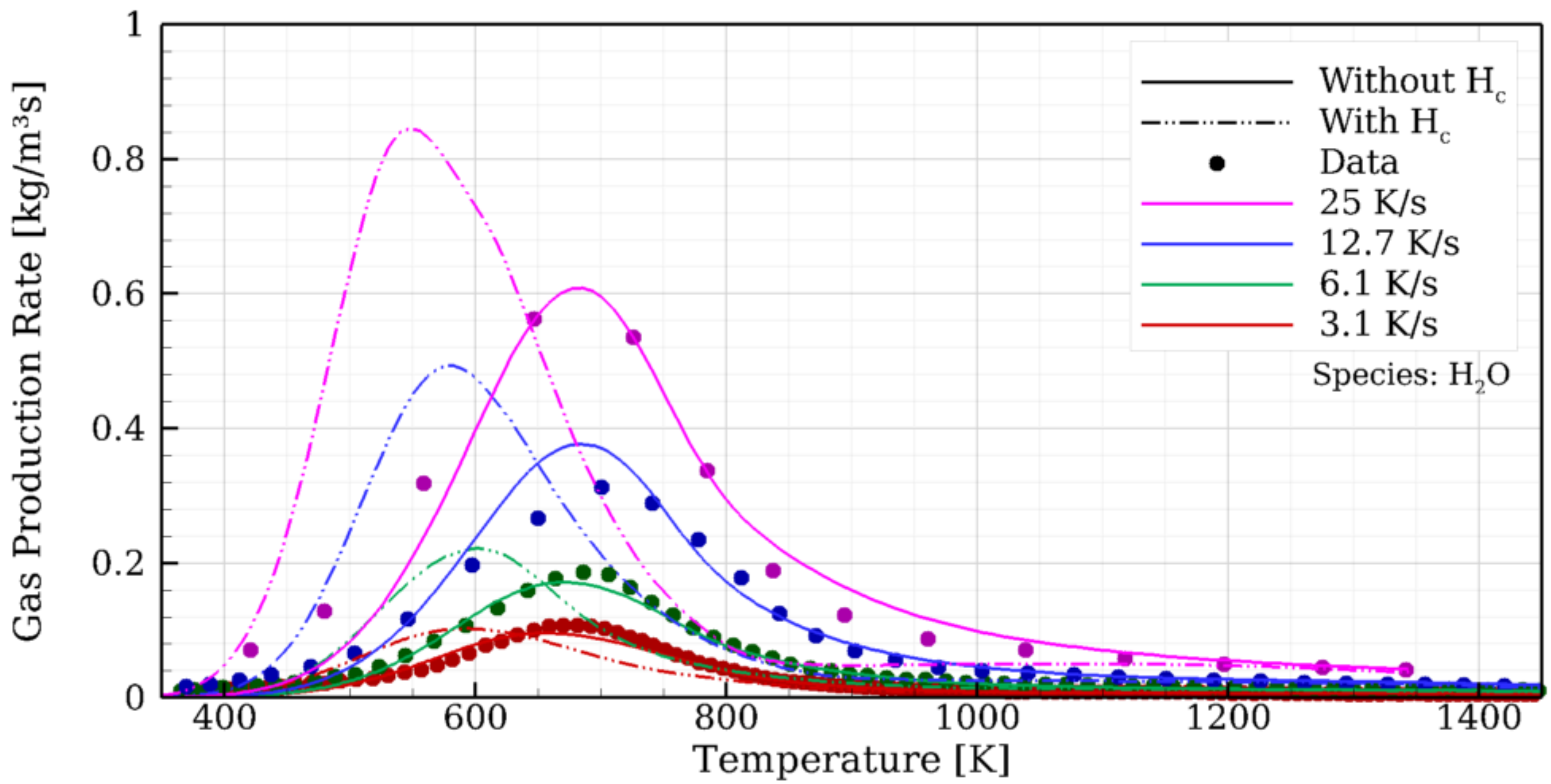

Competitive Mechanism In-Work

- Treating carbon rings (R) and bridges (B_x) or groups (G_x) attached to rings as "species"
  - Initial composition of bridge and group species defined by solution of linear system constrained by ring sites, elemental composition, and impurity levels
  - Standard Arrhenius model for each reaction with user-specified reaction order
  - Some species grouped into single reaction as it is noticed that they behave similarly in test data
- Mechanism initially based on that of Trick and Saliba, but have modified it based on observations of Bessire and Minton
  - Currently missing thermo data for species:
    - Dimethyl Phenol (Xylenol)
    - Trimethyl Phenol
    - Treating these species as Cresol for now
- Do not have a gas-phase reaction mechanism including larger hydrocarbons to model homogeneous reactions in pyro gas

Cross-Linking

$$2G_{OH} \rightarrow B_O + H_2O\bullet$$
$$B_{CH_2} + G_{OH} \rightarrow B_{CH} + H_2O\bullet$$
$$G_{OH} + G_H \rightarrow B_c + H_2O\bullet$$

Condensation

$$2R + 2G_{OH} + B_{CH2} + 8G_H \rightarrow \text{Dibenzofuran} + H_2O\bullet$$
$$\text{Dibenzofuran} \rightarrow H_2O + CO + CH_4 + H_2$$
$$2R + B_O + 10G_H \rightarrow \text{Xanthene} + 2H\bullet$$
$$\text{Xanthene} \rightarrow H_2O + CO + CH_4 + H_2$$

Polymer Scission

$$xR + xB_{CH_2} + xG_{OH} + xG_H + xH\bullet \rightarrow x\text{Phenol} + x\text{n-methyl Phenol} + xCO_2$$
$$xR + xB_{CH_2} + xB_O + xB_{CH} + xG_H + xH\bullet \rightarrow x\text{Toluene} + x\text{Xylene}$$
$$R + B_{CH_2} + 5G_H + 3H\bullet \rightarrow G_H + \text{Benzene} + CH_4$$

Graphitization

$$B_{CH_2} + H_2O\bullet \rightarrow B_c + CO + 4H\bullet$$
$$B_O + B_{CH_2} \rightarrow 2B_c + CO + 2H\bullet$$
$$2B_{CH} \rightarrow \frac{1}{3}R + 2H\bullet$$
$$2G_H \rightarrow B_C + 2H\bullet$$

Impurity Terminators

$$G_{CH_2OH} + H_2O\bullet \rightarrow CO_2 + 2H_2$$
$$G_{CH_2OH} + H_2O\bullet \rightarrow CO + H_2 + H_2O$$

Radical Cleanup

$$2H\bullet \rightarrow H_2$$
$$H_2O\bullet \rightarrow H_2O$$

Trick, K. A., & Saliba, T. E. (1995). Mechanisms of the pyrolysis of phenolic resin in a carbon/phenolic composite. *Carbon*, *33*(11), 1509–1515. http://doi.org/10.1016/0008-6223(95)00092-R

Conclusions

- 3D thermal analysis of experiments suggest that spatial non-uniformities could be present and could be affecting the data interpretation
  – Results have been shared with the experimental team, and an alternative configuration is being developed for future tests

- Method has been developed to make use of existing data in mechanism development, although a number of modeling assumptions do qualify the results
  – TC wire/PICA contact conductance is likely the largest remaining uncertain parameter
  – Reradiation environment, material electrical conductivity, heat of pyrolysis, shielding of species from mass spectrometer potentially also contribute

- Initial work using a derived non-competitive reaction mechanism are being used to further development of homogeneous reaction mechanism while a competitive pyrolysis mechanism is being developed

Backup

Decomposition Model Form

- PICA will be modeled as a perfect mixture of constituents, defined by apparent density: $\bar{\rho} = \sum_{k=1}^{nc} \bar{\rho}_k \quad [\mathrm{kg}/\mathrm{m}^3]$
- An arbitrary number of reactions may be defined, each with the general form:

$$\sum_{i=1}^{ns} \nu'_{ij}\mathcal{A}_i + \sum_{k=1}^{nc} \mu'_{kj}\mathcal{B}_k \rightleftharpoons \sum_{i=1}^{ns} \nu''_{ij}\mathcal{A}_i + \sum_{k=1}^{nc} \mu''_{kj}\mathcal{B}_k$$

$\mathcal{A}_i$: Gaseous species

$\mathcal{B}_k$: Condensed constituent

$$\text{Gaseous species source term } [\mathrm{kg_i}/\mathrm{m}^3\cdot\mathrm{sec}]\text{: } \dot{\omega}_{g_i}^{rxn} = \frac{M_i}{1000}\sum_{j=1}^{nr}\left(\nu''_{ij} - \nu'_{ij}\right)\tau_j$$

$$\text{Condensed constituent source term } [\mathrm{kg_k}/\mathrm{m}^3\cdot\mathrm{sec}]\text{: } \dot{\omega}_{c_k}^{rxn} = \frac{M_k}{1000}\sum_{j=1}^{nr}\left(\mu''_{kj} - \mu'_{kj}\right)\tau_j$$

$$\text{Reaction rate of progress } [\mathrm{mol}/\mathrm{m}^3\mathrm{sec}]\text{: } \tau_j = k_{f_j}\left[\prod_{i=1}^{ns}\tilde{\rho}_i^{\theta'_{g,ij}}\prod_{k=1}^{nc}[\bar{\rho}_k]^{\theta'_{c,kj}}\right] - k_{b_j}\left[\prod_{i=1}^{ns}\tilde{\rho}_i^{\theta''_{g,ij}}\prod_{k=1}^{nc}[\bar{\rho}_k]^{\theta''_{c,kj}}\right]$$

$$\text{Forward reaction (Arrhenius) rate } [\mathrm{mol}/\mathrm{m}^3\cdot\mathrm{sec}]\text{: } k_{f_j} = A_j T^{\theta_{T,j}}\exp\left(\frac{-\theta_{d_j}}{T}\right)$$

$$\text{Backward reaction rate } [\mathrm{mol}/\mathrm{m}^3\cdot\mathrm{sec}]\text{: } k_{b_j} = \text{not yet defined}$$

- For a single constituent decomposing to gas, this simplifies to:

$$\frac{\partial\rho_k}{\partial t} = -\frac{M_k}{1000}\left(AT^{\psi}e^{-Ea/T}\right)\tilde{\rho}_k^{\theta'}$$

A : Rate constant

ψ : Temperature order

Ea : Activation temperature

θ' : Reaction order

- Integrating reactions in time from an initial apparent density vector yields TGA and species production rates

In-Work Reaction Mechanism

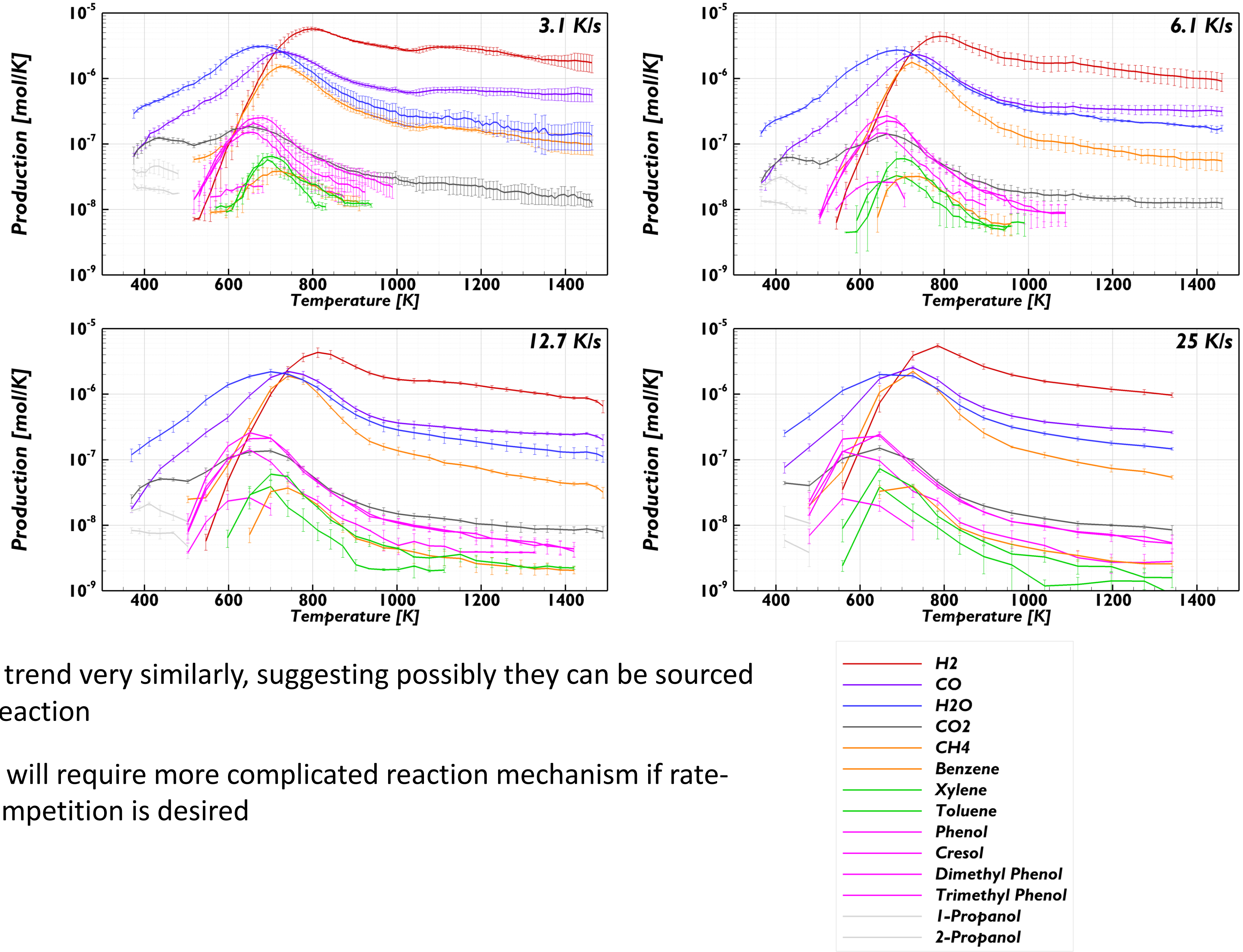

- Many species trend very similarly, suggesting possibly they can be sourced by the same reaction
- Other species will require more complicated reaction mechanism if rate-dependent competition is desired

Constituent Species Nomenclature

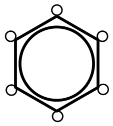
: R : Carbon ring (open circles denote arbitrary molecule bonded to carbon atom)

: B_H : Hydrogen atom (noted as empty spot on carbon ring)

: B_{OH} : Hydroxyl group

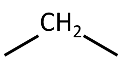

: B_{CH_2} : Methylene bridge

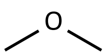

: B_O : Ether bridge

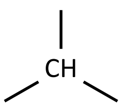

: B_{CH} : CH bridge

— : B_C : Direct carbon bond

H· : $H\bullet$: Condensed hydrogen “radical”

$H_2O\cdot$: $H_2O\bullet$: Condensed water “radical”

B_c will not be tracked as a species (no mass), it is used in balancing equations and is essentially a sink for bridge sites

Intermolecular Dehydration

$$2B_{OH} \rightarrow B_O + H_2O\bullet$$

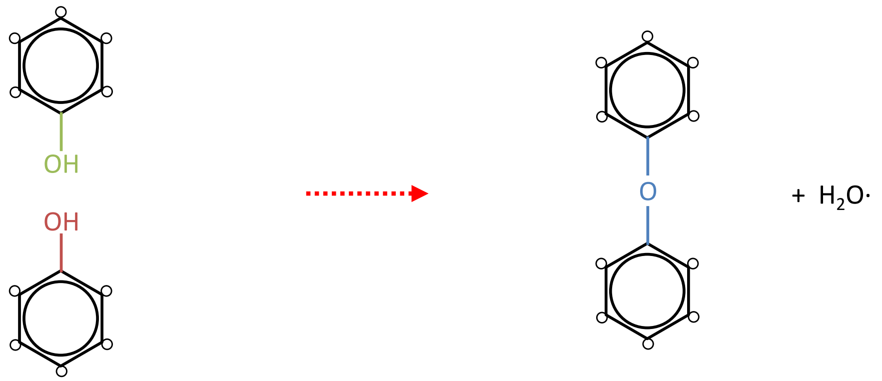

$$B_{CH_2} + B_{OH} \rightarrow B_{CH} + H_2O\bullet$$

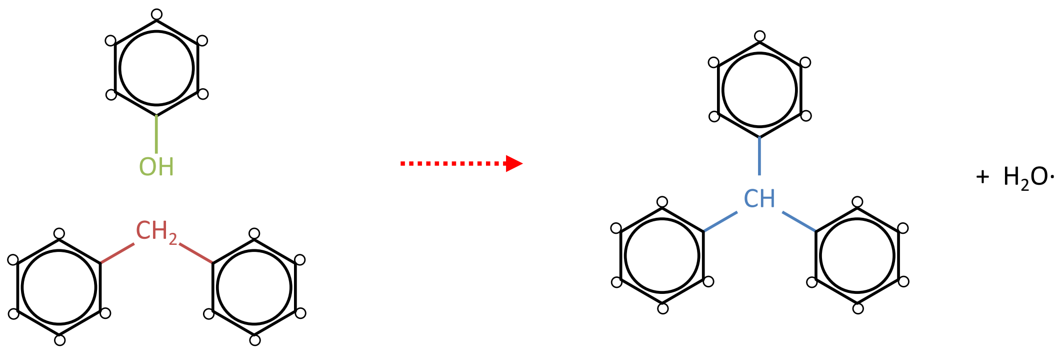

Intramolecular Dehydration

$$2R + 2B_{OH} + B_{CH2} + 8B_H \rightarrow \text{Dibenzofuran} + H_2O\bullet$$

$$2R + B_O + 10B_H \rightarrow \text{Xanthene} + 2H\bullet$$

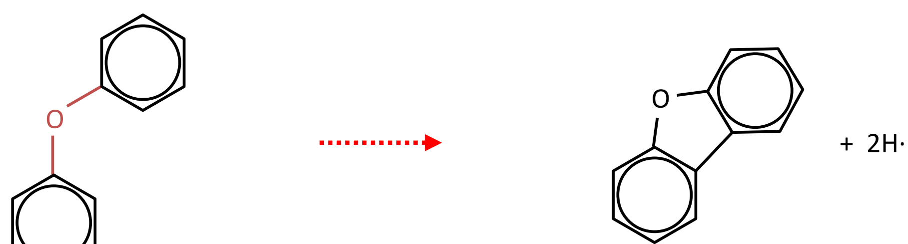

Hydrogen Radical Production

$$B_{CH_2} + H_2O\bullet \rightarrow B_c + CO + 4H\bullet$$

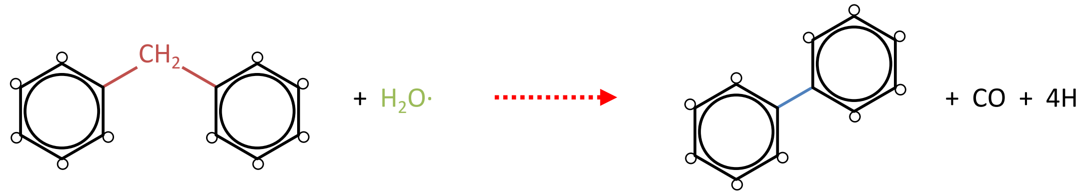

$$B_O + B_{CH_2} \rightarrow 2B_c + CO + 2H\bullet$$

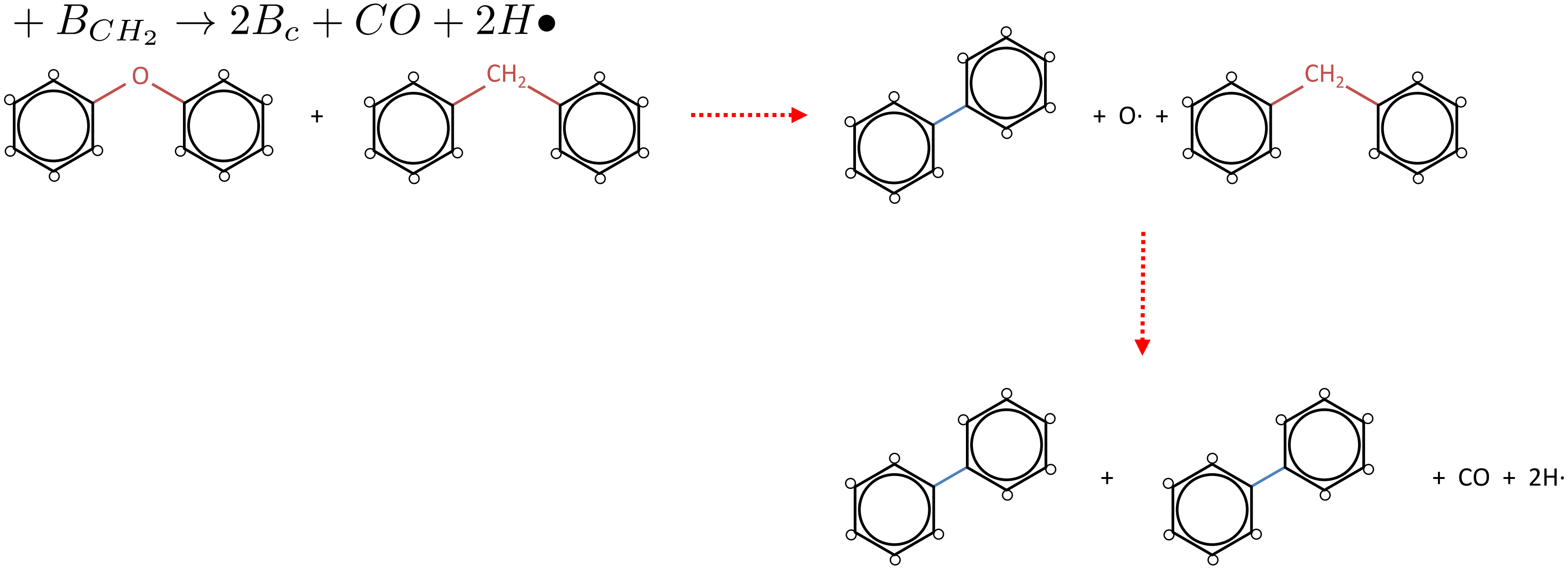

Hydrogen Abstraction

$$2B_{CH} \rightarrow \frac{1}{3}R + 2H\bullet$$

Additional 1/3 R formed since 4 of 6 atoms in new R already present in R molecule

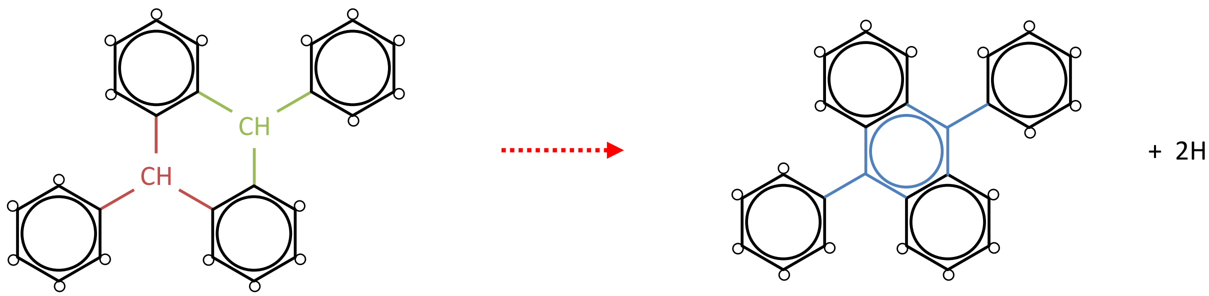

$$2B_{H} \rightarrow B_{C} + 2H\bullet$$

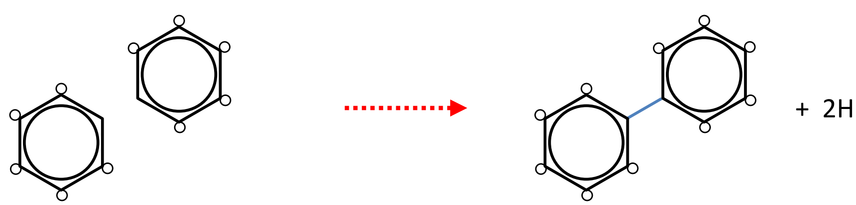

Polymer Scission with Hydroxyl Groups

$$R + B_{OH} + 3B_H + 2H\bullet \rightarrow \text{Phenol}$$

$$R + B_{OH} + B_{CH_2} + 3B_H + 2H\bullet \rightarrow \text{Cresol}$$

$$R + B_{OH} + 2B_{CH_2} + 3B_H + 2H\bullet \rightarrow \text{Dimethyl Phenol}$$

$$R + B_{OH} + 3B_{CH_2} + 2B_H + 3H\bullet \rightarrow \text{Trimethyl Phenol}$$

$$\text{Impurity Terminators} \rightarrow CO_2$$

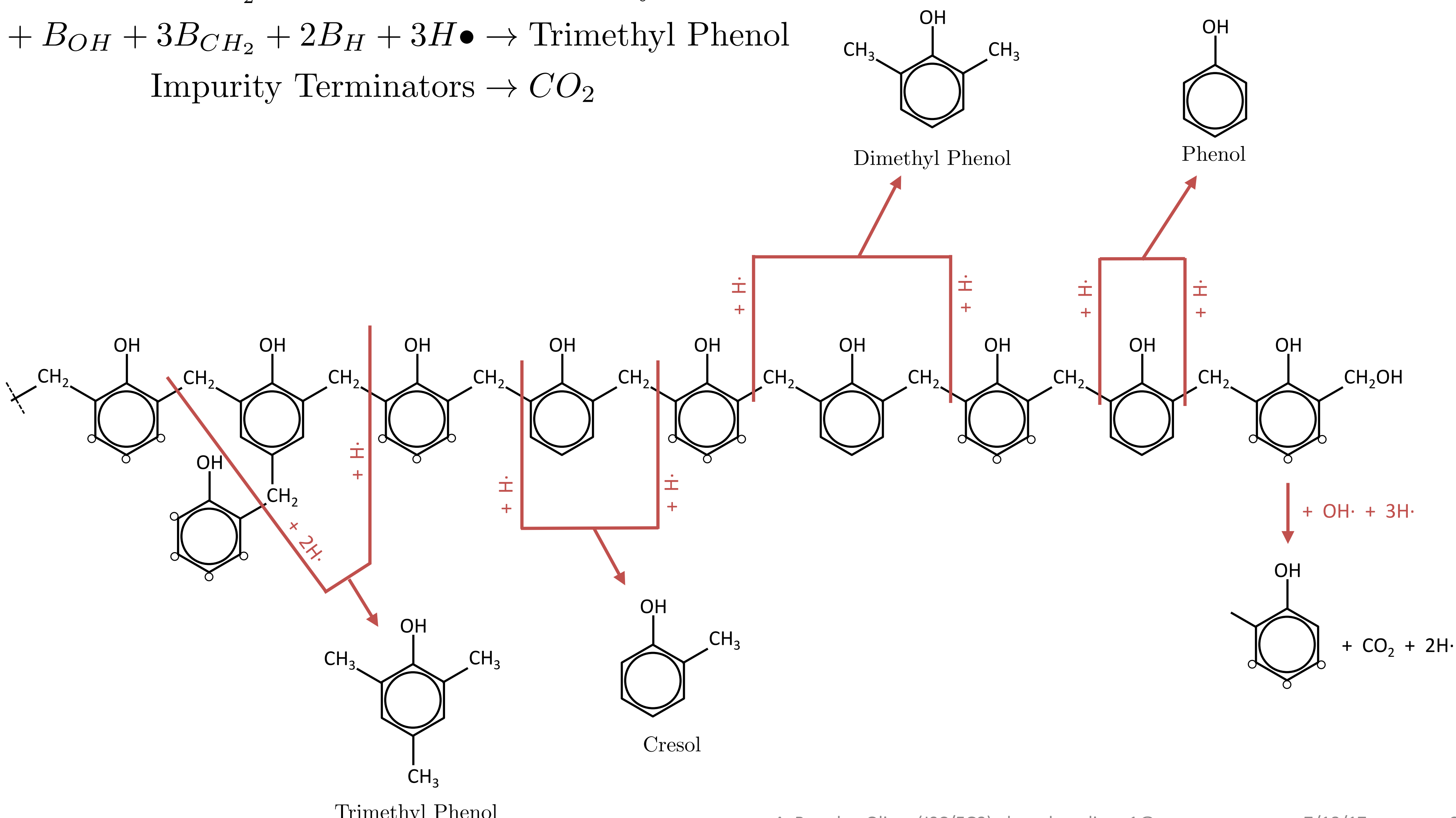

Polymer Scission without Hydroxyl Groups

$$R + B_O + 2B_{CH_2} + 3B_H + 3H\bullet \rightarrow \text{Toluene}$$
$$R + B_O + 2B_{CH_2} + 3B_H + 3H\bullet \rightarrow \text{Xylene}$$

$$R + B_{CH} + 2B_{CH_2} + 3B_H + 4H\bullet \rightarrow \text{Toluene}$$
$$R + B_{CH} + 2B_{CH_2} + 3B_H + 4H\bullet \rightarrow \text{Xylene}$$

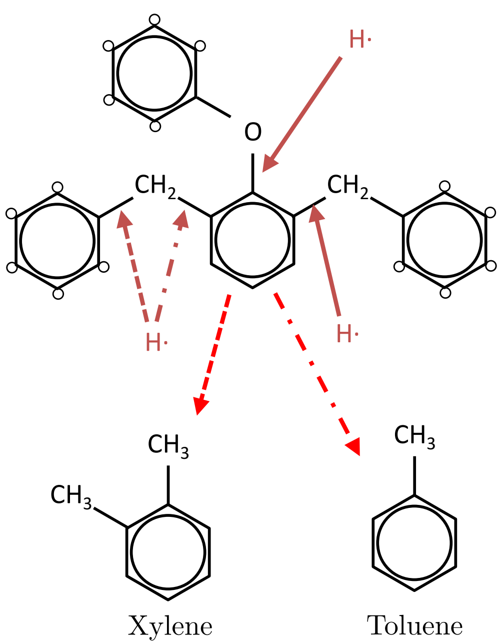

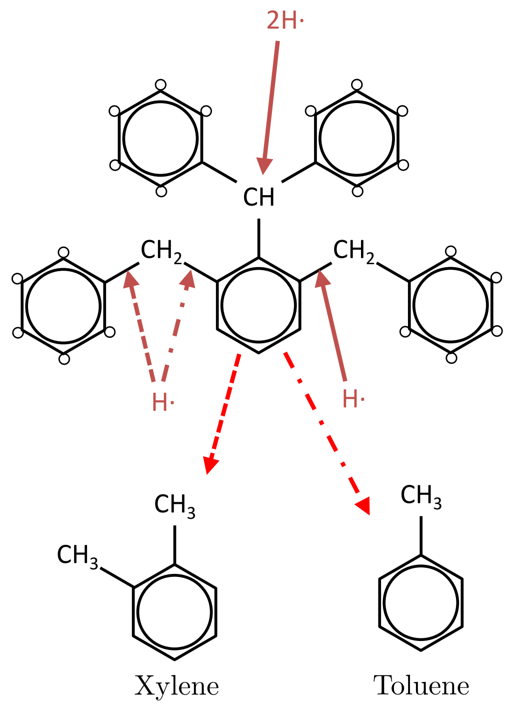

$$R + B_{CH_2} + 5B_H + 2H\bullet \rightarrow \text{Benzene} + CH_4$$

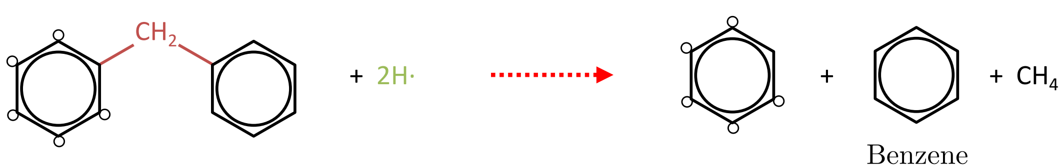

Stoichiometry

- Dibenzofuran: (breaks down early)
  - H_2: 1.0, CH_4: 0.08, CO: 0.21, H_2O: 0.15
- Xanthene: (breaks down later)
  - H_2: 1.0, CH_4: 0.06, CO: 0.3, H_2O: 0.15
- Scission w/ hydroxyl groups:
  - Phenol: 1.0, Cresol: 2.0, CO_2: 1.0
  - (plot does not group dimethylphenol into cresol like it should)
- Scission w/o hydroxyl groups:
  - Xylene: 1.0, Toluene: 2.0

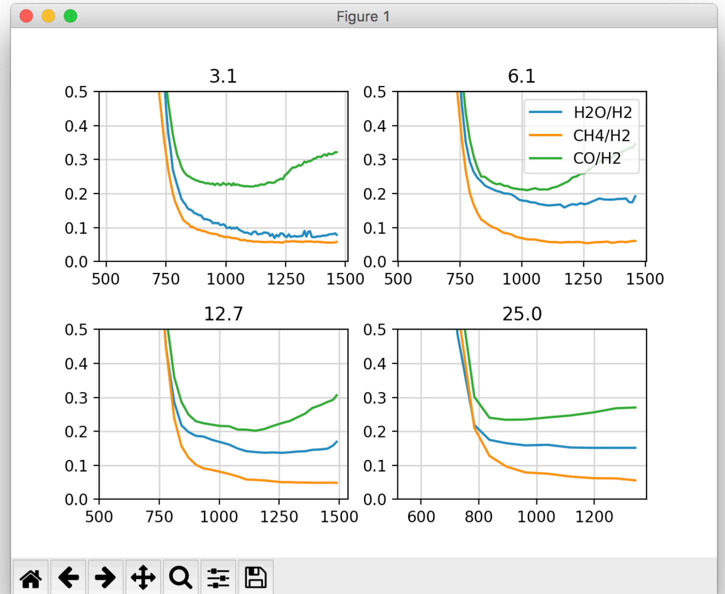

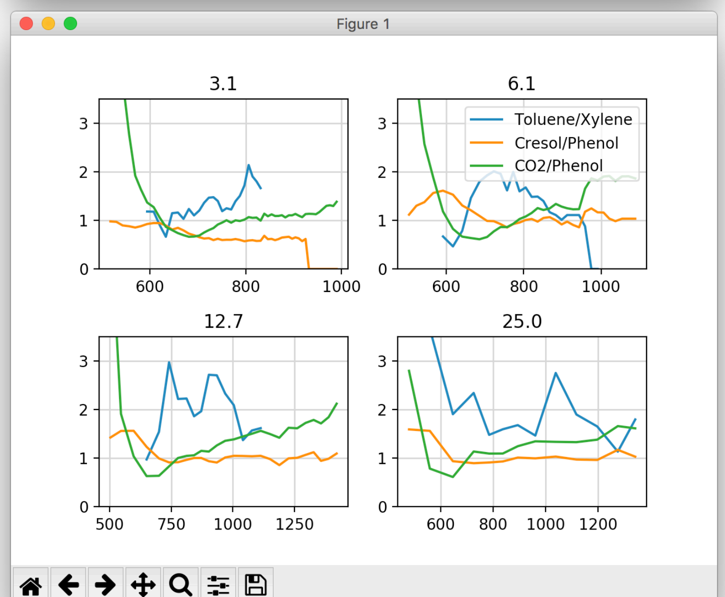

Twisted TC Analysis

- CHAR analysis:
  - Added Seebeck term to CHAR thermoelectric system, assuming electric field is steady
  - Considered square and round wire cross sections
- Effective junction appears to be very close to the exposed surface of the sample

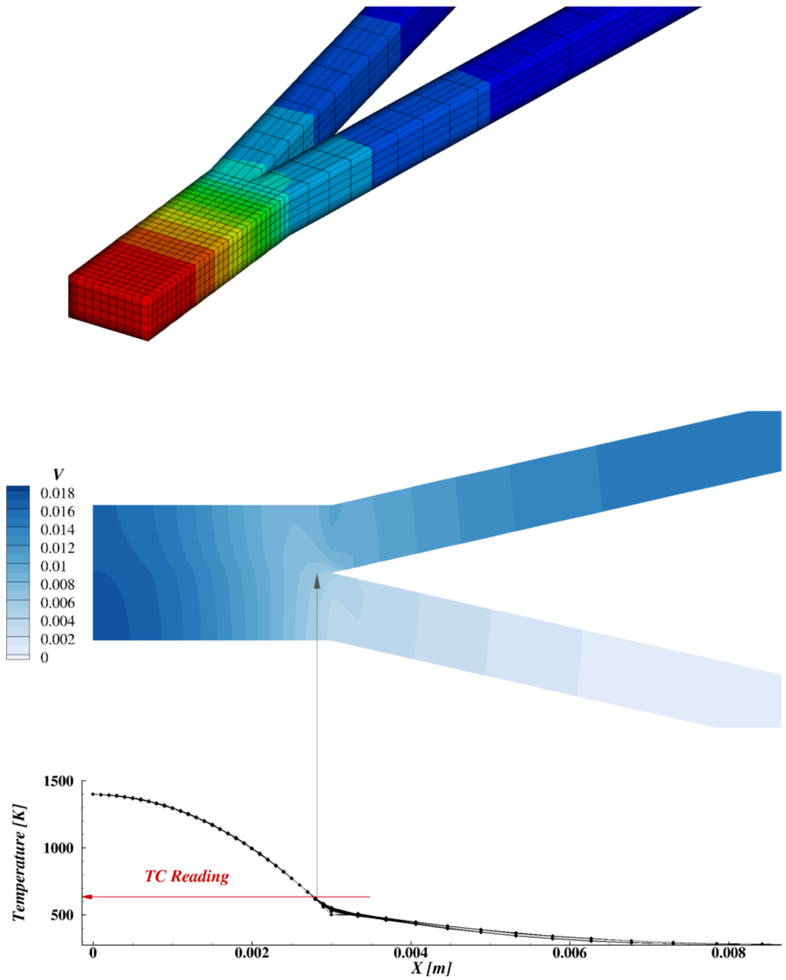

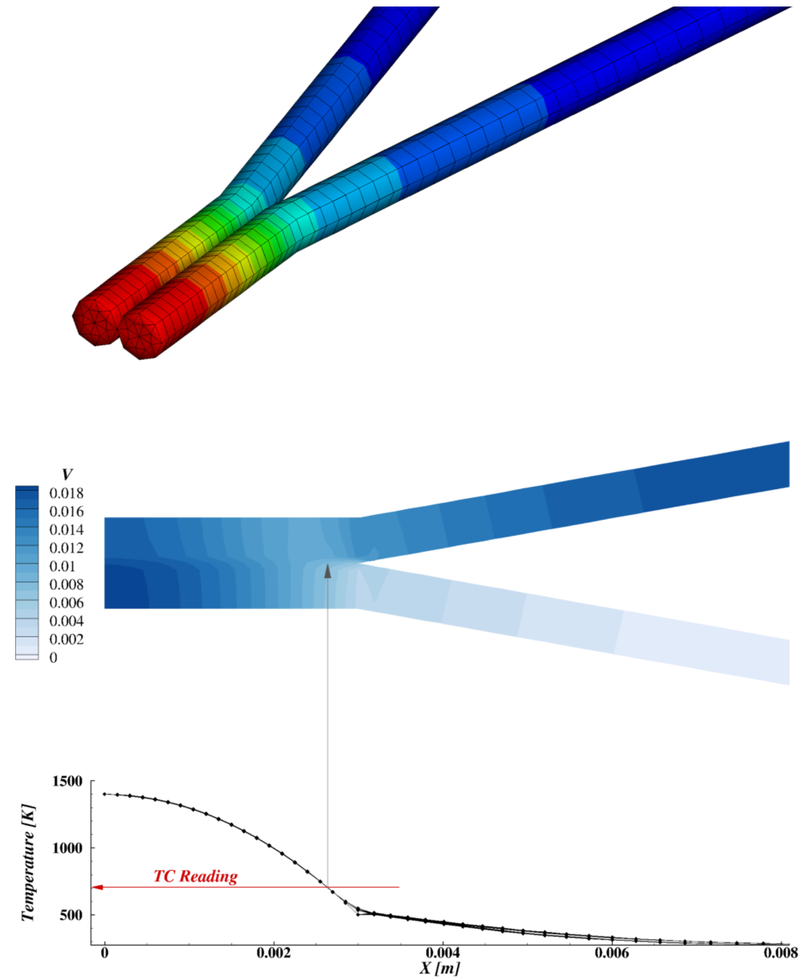

Twisted TC Analysis

- CHAR analysis:
  - Added Seebeck term to CHAR thermoelectric system, assuming electric field is steady
  - Considered square and round wire cross sections
- Effective junction appears to be very close to the exposed surface of the sample